A New Infrared Electronic Transition of the Oxidized Primary Electron Donor in Bacterial Reaction Centers: A Way To Assess Resonance Interactions between the Bacteriochlorophylls†

Jacques Breton,*,‡ Eliane Nabedryk,‡ and William W. Parson*,§

SBE/DBCM, CEN-Saclay, 91191 Gif-sur-Yvette Cedex, France, and Department of Biochemistry, University of Washington, Seattle, Washington 98195

Received March 4, 1992; Revised Manuscript Received May 13, 1992

ABSTRACT: The primary electron donor in the reaction center of purple photosynthetic bacteria consists of a pair of bacteriochlorophylls (P_L and P_M). The oxidized dimer (P^+) is expected to have an absorption band in the mid-IR, whose energy and dipole strength depend in part on the resonance interactions between the two bacteriochlorophylls. A broad absorption band with the predicted properties was found in a previously unexplored region of the spectrum, centered near 2600 cm^{-1} in reaction centers of *Rhodobacter sphaeroides* and several other species of bacteria that contain bacteriochlorophyll *a*, and near 2750 cm^{-1} in *Rhodopseudomonas viridis*. The band is not seen in the absorption spectrum of the monomeric bacteriochlorophyll cation in solution, and it is missing or much diminished in the reaction centers of bacterial mutants that have a bacteriopheophytin in place of either P_L or P_M. With the aid of a relatively simple quantum mechanical model, the measured transition energy and dipole strength of the band can be used to solve for the resonance interaction matrix element that causes an electron to move back and forth between P_L and P_M, and also for the energy difference between states in which a positive charge is localized on either P_L or P_M. (The absorption band can be viewed as representing a transition between supermolecular eigenstates that are obtained by mixing these basis states.) The values of the matrix element obtained in this way agree reasonably well with values calculated by using semiempirical atomic resonance integrals and the reaction center crystal structures. The two basis states with localized charges appear to differ substantially in energy, so that the charge distribution in P^+ is decidedly asymmetrical. The energy and relative strength of the absorption band change very little with temperature, indicating that the distance between P_L and P_M probably does not decrease significantly when reaction centers are cooled to cryogenic temperatures.

Now that the structure of the photosynthetic bacterial reaction center (RC)[1] is known at atomic resolution (Deisenhofer et al., 1985; Allen et al., 1987; Yeates et al., 1988; Tiede et al., 1988; Deisenhofer & Michel, 1989a,b; Feher et al., 1989; Chang et al., 1991; El-Kabbani et al., 1991), the challenge has arisen of relating the structure to the RC's remarkable spectroscopic and kinetic properties (Breton & Verméglio, 1988; Michel-Beyerle, 1990). Of pivotal importance here is an exploration of the special pair of bacteriochlorophyll (BChl) molecules that serve as the primary electron donor (P). The two BChls of P (P_L and P_M) sit close together in the RC, with their molecular planes nearly parallel and separated by about 3.3 Å. They are related by a noncrystallographic axis of 2-fold symmetry that also relates the two other, more widely separated BChls of the RC, the two bacteriopheophytins (BPhs), the two quinones (Q_A and Q_B), and homologous amino acid residues in the two main polypeptides. When the RC is excited with light, the excitation energy moves to P within about 0.1 ps (Breton et al., 1986). The excited dimer (P^*) then transfers an electron to one of the BPhs (H_L) in about 3 ps, possibly by way of an intervening BChl (B_L) (Woodbury et al., 1985; Martin et al., 1986; Kirmaier & Holten, 1987; Holzapfel et al., 1990). The electron-transfer reaction generates a radical pair ($P^+H_L^-$), which decays in about 200 ps by the movement of an electron from H_L^- to Q_A.

The intense, long-wavelength absorption band of the RC must be due mainly to the special pair of BChls, because it bleaches reversibly when P is raised to an excited state or is oxidized to the radical cation (P^+). This band is shifted markedly to the red, compared to the corresponding "Q_y" band of monomeric BChl in vitro. Whereas BChl-*a* in methanol or pyridine absorbs near 770 nm, the absorption spectrum of *Rhodobacter sphaeroides* RCs peaks near 865 nm. In *Rhodopseudomonas viridis* RCs, which contain BChl-*b*, the long-wavelength band is near 960 nm, compared to 790 nm for monomeric BChl-*b* in vitro. The red shift of the absorption band becomes even larger at cryogenic temperatures, in parallel with an increase in the rate of the initial electron-transfer reaction (Kirmaier & Holten, 1988). In addition, the long-wavelength absorption band exhibits a characteristic Stark effect (Lockhart & Boxer, 1987, 1988; Lösche et al., 1987) and circular dichroism (Philipson & Sauer, 1973). P^+ also has an unusual absorption spectrum, including a band at 1250 nm in *Rb. sphaeroides* or 1320 nm in *Rp. viridis*, where the corresponding radical of monomeric BChl has little absorbance (Parson & Cogdell, 1975).

† This work was supported by a Human Frontier Science Program grant to J.B. and NSF Grant DMB-9111599 to W.W.P.

‡ SBE/DBCM, Bât. 532, CEN-Saclay, 91191 Gif-sur-Yvette Cedex, France.

§ Dept. of Biochemistry, SJ-70, University of Washington, Seattle, WA 98195.

[1] Abbreviations: cyt, cytochrome; BChl, bacteriochlorophyll; BPh, bacteriopheophytin; FTIR, Fourier transform infrared; fwhm, full width at half-maximum amplitude; HOMO, highest occupied molecular orbital; P, primary electron donor; P_L and P_M, the two BChls that make up P; Q_A and Q_B, primary and secondary quinone electron acceptors; B_L and H_L, BChl and BPh molecules located between P and Q_A; RC, reaction center.

0006-2960/92/0431-7503$03.00/0

These spectroscopic properties probably arise mainly from interactions between BChls P_L and P_M. Although electrostatic interactions with the surrounding protein could, in principle, shift the Q_y band of BChl to either the red or the blue (Eccles & Honig, 1983), the crystal structures of the RC reveal no ionizable amino acid residues close enough to P to have an appreciable effect. Interactions of P with the other two BChls or the two BPhs undoubtedly contribute to the details of the absorption and CD spectra but again probably are relatively weak (Breton, 1985; Parson & Warshel, 1987; Scherer & Fischer, 1991). Attention therefore has focused on the excitonic interactions between P_L and P_M, and on the resonance interactions that mix exciton states with charge-transfer states of the dimer. Models that consider exciton interactions alone appear to be unsatisfactory because they fail to explain the large Stark effect measured in the long-wavelength band. In addition, calculations based on the crystallographic structure indicate that such models have difficulty in accounting quantitatively for the red shift of the band (Parson & Warshel, 1987; Scherer & Fischer, 1991). The absorption and CD spectra and the Stark effect can all be explained reasonably well by semiempirical molecular orbital treatments that include resonance interactions with charge-transfer states (Warshel & Parson, 1987; Parson & Warshel, 1987; Won & Friesner, 1988a; Friesner & Won, 1989; Hanson, 1988; Eccles et al., 1988; Thompson & Zerner, 1990; Scherer & Fischer, 1989a, 1991). However, differences of opinion remain as to the magnitudes of the resonance energies that are involved. Many of the spectroscopic properties can be rationalized either by strong resonance interactions with a charge-transfer state that is considerably higher in energy than the lowest exciton state or by weaker interactions with a charge-transfer state that lies closer in energy.

Neither the resonance energies nor the charge-transfer transition energies of P are directly measurable experimentally, and attempts to calculate them on the basis of the crystal structure are subject to a variety of uncertainties. For example, although P_L and P_M have overlapping macrocyclic rings, calculations of their resonance interactions still require evaluating atomic resonance integrals for many pairs of atoms that are separated by distances exceeding 4 Å. The semiempirical atomic resonance integrals that enter into such calculations have been calibrated well only for shorter distances. It would, therefore, be useful to have an independent experimental property that reflects the magnitude of the resonance interactions between the two BChls.

The need for new ways to evaluate resonance interactions in the RC becomes increasingly pressing when one considers the kinetics of the initial electron-transfer reaction. The interaction matrix elements that mix P* with radical pair states such as $P^+B_L^-$ and $P^+H_L^-$ are closely related to the matrix elements that mix charge-transfer states of P into P*, and they can be expressed similarly in terms of atomic resonance integrals (Kuhn, 1986; Parson et al., 1987; Källebring & Larsson, 1987; Warshel et al., 1988; Scherer & Fischer, 1989a,b; Plato & Winscom, 1988). However, because the distances separating P from B_L and H_L are outside the range for which the atomic resonance integrals have been calibrated, the electron-transfer matrix elements cannot presently be evaluated with confidence. The values that have been calculated to date are somewhat too small to account for the measured kinetics of the reaction in *Rp. viridis*, and much too small in *Rb. sphaeroides* (Parson et al., 1987; Warshel et al., 1988; Scherer & Fischer, 1989a,b; Plato & Winscom, 1988). The uncertainties of such calculations present an obstacle to resolving the question of whether the initial electron-transfer reaction occurs by superexchange or by the formation of $P^+B_L^-$ as a distinct intermediate.

Katz et al. (1979) and Parson et al. (1990) have pointed out that P^+ should have a series of eigenstates whose separations depend, in part, on resonance interactions between P_L and P_M. These states can be viewed as linear combinations of basis states in which the positive charge and an unpaired electron are localized on either P_L or P_M alone. Again, the off-diagonal matrix elements that mix such basis states are closely related to the matrix elements that mix charge-transfer states with exciton states of P. Transitions among the eigenstates of P^+ should give rise to absorption bands in the mid-IR region of the spectrum. In the present paper, we describe a new absorption band that appears to represent such a transition, and we show how measurements of its energy and dipole strength can be related to the calculated resonance energies.

MATERIALS AND METHODS

Reaction centers of *Rb. sphaeroides* R-26 and *Rp. viridis* were purified in lauryldimethylamine oxide by standard procedures (Feher & Okamura, 1978; Clayton & Clayton, 1978), and the detergent was exchanged for sodium cholate (0.5%) on a diethylaminoethyl-Sepharose column. The cholate concentration was decreased by repetitive steps of dilution with deionized water and concentration on an Amicon filter until the RCs started to aggregate. Chromatophores from *Rb. sphaeroides*, *Rp. viridis*, *Rhodobacter capsulatus*, *Rhodospirillum rubrum*, *Chromatium vinosum*, and *Chloroflexus aurantiacus* were prepared by French-press treatment followed by density-gradient centrifugation. For study, samples were dried on CaF_2 disks under a flow of N_2. The water content of the specimen was controlled by measuring the ratio of the absorbances at 3300 and 1650 cm^{-1}, which was kept between 0.4 and 0.8. The dried film was sealed in an air-tight CaF_2 cuvette and cooled in a temperature-regulated cryostat.

Spectroscopic measurements were performed with a Nicolet 60SX FTIR spectrometer that allowed optimization of the radiation source (tungsten lamp or globar), beam-splitter (CaF_2 or KBr) and detector (Si or HgCdTe) for different regions of the spectrum. The tungsten–CaF_2–Si configuration was used between 13 500 and 9000 cm^{-1}, tungsten–CaF_2–HgCdTe between 11 500 and 1800 cm^{-1}, and globar–KBr–HgCdTe between 4000 and 1200 cm^{-1}. In the first and second configurations, a KRS-5 filter and a 50%-transmitting mesh were placed in front of the sample to decrease the actinic effect of the measuring beam; in the third configuration, the sample was protected by a germanium filter. The spectral resolution was 16 cm^{-1} in the first configuration, either 16 or 4 cm^{-1} in the second, and 4 cm^{-1} in the third. To photooxidize P, the sample was illuminated by an additional beam from a tungsten lamp equipped with colored and neutral-density filters immersed in 3 cm of water. The overlapping spectral ranges accessible with the three configurations allowed the amplitudes of the measured absorbance changes to be corrected for differences in the actinic effects of the measuring beams. A KRS-5 wire grid polarizer was placed in the measuring beam for measurements of the linear dichroism of the absorbance changes (Thibodeau et al., 1991).

RESULTS

Figures 1a and 2a show the absorption spectrum of a film of *Rb. sphaeroides* RCs at 260 K over the overlapping frequency ranges from 13 500 to 2000 cm^{-1} and from 4000

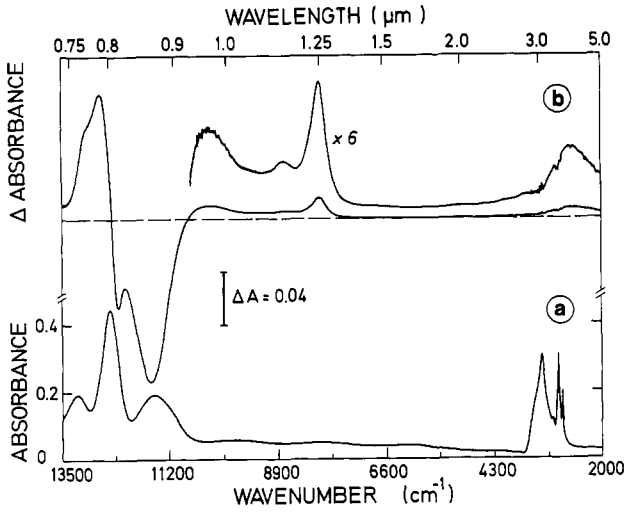

FIGURE 1: Near-IR absorption spectrum (a) and light minus dark ($P^+Q_A^-/PQ_A$) difference spectrum (b) of a film of *Rb. sphaeroides* R26 RCs at 260 K: spectral resolution, 16 cm^{-1} above 9000 cm^{-1} and 4 cm^{-1} below 9000 cm^{-1}. In (a), 128 interferograms were coadded. In (b), 60 light minus dark cycles of 128 interferograms were averaged.

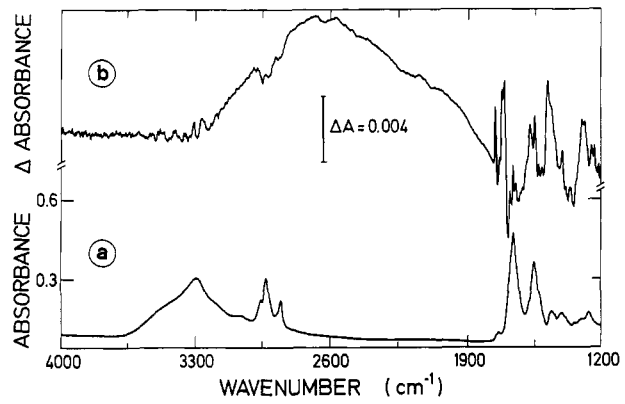

FIGURE 2: Mid-IR absorption spectrum (a) and light minus dark ($P^+Q_A^-/PQ_A$) difference spectrum (b) of the same film of *Rb. sphaeroides* R26 RCs as used in Figure 1: temperature, 260 K; resolution, 4 cm^{-1}. In (a), 128 interferograms were coadded. In (b), 100 light minus dark cycles of 128 interferograms were averaged.

to 1200 cm^{-1}. The spectrum in the near-IR region (Figure 1a) includes the well-characterized bands at 860, 800, and 760 nm, which are due mainly to P, the other two BChls, and the BPhs, respectively. In the mid-IR (Figure 2a), the main bands represent the protein amide A (3300 cm^{-1}), amide I (1650 cm^{-1}), amide II (1550 cm^{-1}), CH_3 (2960 cm^{-1}), and CH_2 (2930 and 2850 cm^{-1}) vibrational modes.

The light minus dark difference spectrum measured upon photooxidation of P is shown in Figures 1b and 2b. The difference spectrum is dominated by the bleaching of the band at 860 nm, a blue shift of the 800-nm band, and the formation of a band at 1250 nm. The 1250-nm band has been assigned previously to P^+, although the nature of the transition that it represents has not been entirely clear (Dutton et al., 1975; Parson & Cogdell, 1975; Fajer et al., 1975; Davis et al., 1979). The spectral region extending from 7500 to 4000 cm^{-1} is essentially featureless (Figure 1b). At lower frequencies, in the region of the mid-IR that has been studied most extensively (1800–1200 cm^{-1}), there are a series of small, but highly reproducible absorption changes. These reflect alterations of bond lengths and force constants in the cofactors and adjustments of the interactions between the cofactors and the protein in response to charge separation (Mäntele et al., 1985, 1988, 1990; Nabedryk et al. 1986, 1988, 1990; Buchanan et al., 1990; Thibodeau et al., 1990; Breton et al., 1991a,b). Between 3300 and 1900 cm^{-1}, there is a very broad band centered at 2600 ± 100 cm^{-1}, with a width (fwhm) of 900 ± 100 cm^{-1} and a shoulder in the region of 2100 cm^{-1}. This band has not been described previously other than in recent preliminary communications (Breton et al., 1992; Davis et al., 1992) and is the focus of the present study.

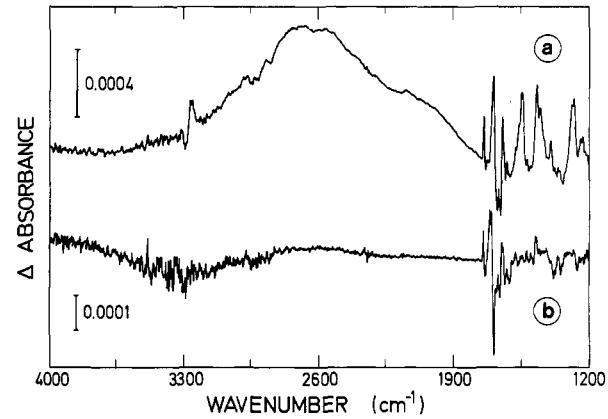

FIGURE 3: Mid-IR light minus dark ($P^+Q_A^-/PQ_A$) difference spectra of films of chromatophores from (a) *Rb. capsulatus* U43 (a strain lacking the B800–850 antenna complex but with wild-type RCs) and (b) the $His^{M200} \rightarrow$ Leu heterodimer RC mutant strain constructed in U43: temperature, 260 K; 200 light minus dark cycles of 128 interferograms were averaged.

The RCs that were used to record these spectra had been treated with *o*-phenanthroline to prevent electron transfer from Q_A^- to Q_B. The light minus dark difference spectrum is therefore a $P^+Q_A^-$ minus PQ_A spectrum (henceforth designated $P^+Q_A^-/PQ_A$). In separate experiments (data not shown), the pure Q_A^-/Q_A difference spectrum was generated as described by Breton et al. (1991a) and was found not to contribute measurably to the 2600-cm^{-1} band. There also was no indication of the band in Q_B^-/Q_B spectra generated as described by Breton et al. (1991b).

A similar broad band around 2600 cm^{-1} is seen in the $P^+Q_A^-/PQ_A$ spectra obtained with chromatophores of *Rb. sphaeroides*, *Rh. rubrum*, *C. vinosum*, *Ch. aurantiacus* (data not shown), and *Rb. capsulatus* (Figure 3a). However, the band is either greatly reduced in amplitude or absent altogether in the $P^+Q_A^-/PQ_A$ spectrum of the $His^{M200} \rightarrow$ Leu mutant of *Rb. capsulatus* (Figure 3b). In this mutant, the loss of the histidine that serves as the axial ligand of BChl P_M causes the BChl be replaced by BPh (Coleman & Youvan, 1990). The very weak absorption band that may be discernible in the 2600-cm^{-1} region in Figure 3b could be due to a small population of RCs in which P retains two BChls in spite of the mutation. Similar results were obtained with the complementary heterodimer mutant, $His^{L173} \rightarrow$ Leu (Coleman & Youvan, 1990), in which P_L is replaced by BPh (data not shown). No new bands were found between 4000 and 8000 cm^{-1} in the $P^+Q_A^-/PQ_A$ spectrum of either mutant. A preliminary discussion of the spectra of the mutant RCs in the region between 1800 and 1200 cm^{-1} has been presented by Breton et al. (1991c) and Nabedryk et al. (1992).

No band comparable to the 2600-cm^{-1} band was found in the $BChl^+/BChl$ difference spectrum generated [as described by Mäntele et al. (1988)] with monomeric BChl-*a* in deuterated tetrahydrofuran.

To investigate whether the 2600-cm^{-1} band might reflect perturbations of hydrogen bonds, RCs were transferred to D_2O and allowed to equilibrate for 3 days in the dark at room temperature before drying. The substitution of D for H had no significant effect on the band.

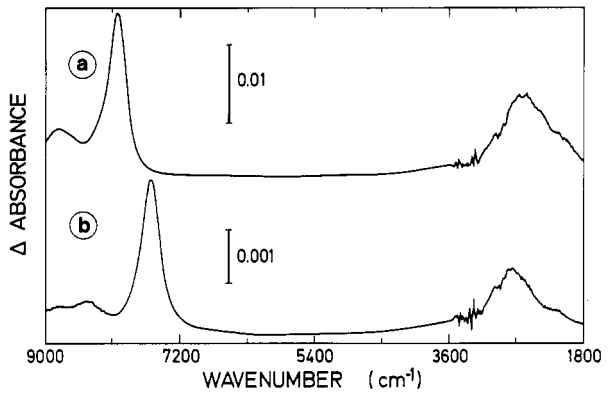

FIGURE 4: Low-temperature (100 K) light minus dark ($P^+Q_A^-/PQ_A$) difference spectra of films of RCs from (a) *Rb. sphaeroides* R26 and (b) *Rp. viridis*. The resolution in (a) was 4 cm^{-1}, and in (b), 16 cm^{-1} above 4000 cm^{-1} and 4 cm^{-1} below 4000 cm^{-1}; 200 light minus dark cycles of 128 interferograms were averaged.

Figure 4a shows a $P^+Q_A^-/PQ_A$ spectrum obtained with *Rb. sphaeroides* RCs at 100 K. The bands at 1250 nm (8000 cm^{-1}) and 2600 cm^{-1} both sharpen with decreasing temperature, but their peak positions are almost unchanged. The peak of the 1250-nm band shifts from 1248 nm at 260 K to 1244 nm at 100 K. This differs from the behavior of the 860-nm band of P, which shifts to markedly longer wavelengths with decreasing temperature. The fwhm of the 2600-cm^{-1} band at 100 K is 730 ± 50 cm^{-1}.

A $P^+Q_A^-/PQ_A$ spectrum obtained with *Rp. viridis* RCs at 100 K is shown in Figure 4b. The positive bands near 1320 nm (7590 cm^{-1}) and 2750 ± 100 cm^{-1} (fwhm = 650 ± 75 cm^{-1}) are similar in shape and position to the corresponding bands seen in *Rb. sphaeroides* (Figure 4a) but are more intense relative to the bleaching of the main near-IR band (990 nm). Recording the $P^+Q_A^-/PQ_A$ spectrum is more difficult with *Rp. viridis* than with *Rb. sphaeroides* because of a faster back-reaction of $P^+Q_A^-$. At higher temperatures, the spectra also can be complicated by absorbance changes resulting from photooxidation of the bound cytochrome. However, the ratio of the amplitudes of the 2750-cm^{-1} and 1320-nm bands appears not to vary greatly with temperature between 100 and 260 K. Separate experiments showed that, like the 2600-cm^{-1} band of *Rb. sphaeroides*, the 2750-cm^{-1} band is practically absent in Q_A^-/Q_A spectra recorded as described by Breton et al. (1991a,b), and also in H_L^-/H_L and $Cyt^+Q_A^-/CytQ_A$ spectra recorded as described by Nabedryk et al. (1986, 1988, 1991).

To determine the dipole strengths of the IR transitions, we compared the areas under the bands in the difference spectra, weighted by the reciprocals of the frequencies, with similarly weighted areas for the bleaching of the main near-IR band of P. The change in dipole strength associated with the latter bleaching was calculated to be 67 ± 4 D^2 in *Rb. sphaeroides* and 90 ± 20 D^2 in *Rp. viridis* by using published extinction coefficients (Straley et al., 1973; Clayton & Clayton, 1978) and taking the refractive index to be 1.3. With *Rb. sphaeroides* RCs at 260 K, we obtained a dipole strength of 7 ± 2 D^2 for the 1250-nm band and 25 ± 8 D^2 for the 2600-cm^{-1} band. For *Rp. viridis* RCs at 100 K, the results were 25 ± 8 D^2 for the 1320-nm band and 85 ± 28 D^2 for the 2750-cm^{-1} band. Apart from the uncertainties in the extinction coefficients of the near-IR bands, the main source of uncertainty in the dipole strengths was the choice of the baseline for measuring the absorbance changes. The stated error bars were obtained by using baselines that clearly led to under- and overestimates of the area under the band.

The linear dichroism of the 2600-cm^{-1} transition was measured with both *Rb. sphaeroides* RCs and *Rp. viridis* chromatophores at 100 K. In both cases, the angle between the transition dipole and the axis of rotational pseudosymmetry of the RC was found to be greater than 60°.

DISCUSSION

The measurements described above show that the absorption spectrum of P^+ includes a broad, and relatively strong absorption band centered near 2600 cm^{-1}. The band appears in the spectra of RCs and chromatophores from a variety of purple bacterial species at both 260 and 100 K, but not in the spectrum of the monomeric BChl cation in vitro. It is lost or much diminished in intensity when the structure of P is modified by a mutation of His L173 or M200. The transition thus appears to be characteristic of the P^+ state in native RCs. The band has previously escaped attention, although its tail was seen as a slope in the apparent baseline of $P^+Q_A^-/PQ_A$ difference spectra in the region between 1800 and 1700 cm^{-1} (Mäntele et al., 1985, 1988, 1990; Nabedryk et al., 1990).

For a number of model systems, hydrogen bonds with large polarizabilites have been reported to be responsible for broad continua of absorption in the region between 1800 and 3000 cm^{-1} (Zundel, 1988). We therefore considered the possibility that the new IR transition arises from a perturbation of H bonds located in the vicinity of the cofactors, such as bonds linking neighboring amino acid side chains or bound water. In this event, the transition should be sensitive to H–D exchange. The observation that the 2600-cm^{-1} transition is unaffected by extensive deuteration of the RC argues against this interpretation. In addition, the crystal structures show that P_L and P_M are surrounded mainly by relatively nonpolar residues, and that they participate in only a few H bonds.

The properties of the 2600-cm^{-1} band are more consistent with an electronic transition of P^+ than with a vibrational transition. To discuss the type of electronic transition that could contribute to the mid-IR region of the spectrum (Katz et al., 1979; Parson et al., 1990), it is convenient to start with a set of π molecular orbitals ϕ_i for the individual BChl molecules, P_L and P_M. Basis states for P^+ then can be written

$$\Phi_i = |\phi_i \prod_{j \neq i} \phi_j \bar{\phi}_j| \qquad \bar{\Phi}_i = |\bar{\phi}_i \prod_{j \neq i} \phi_j \bar{\phi}_j| \tag{1}$$

where the ϕ_j are the filled orbitals of the two BChls. Φ_i represents a radical with an unpaired electron of spin α in orbital ϕ_i; $\bar{\Phi}_i$ represents a similar radical with spin β. Φ_i and $\bar{\Phi}_i$ are degenerate in the absence of a magnetic field, and interconversions between them are formally forbidden. We therefore need to consider only states with a fixed spin of either α or β. For the most important such basis states, the half-filled orbital ϕ_i is the highest normally occupied orbital (HOMO) of either P_L or P_M [ϕ_2 in the four-orbital model of porphyrins (Gouterman, 1959; Warshel & Parson, 1987)]. We will refer to these two states as P_L^+ and P_M^+ and will restrict ourselves here to this simple set.

P_L^+ and P_M^+ are not stationary states, because resonance interactions cause an electron to move back and forth rapidly between the two molecules. The matrix elements for these interactions can be evaluated by expressing the molecular orbitals in terms of atomic p_z orbitals:

$$\phi_i = \sum_s v_s^i \chi_s \tag{2}$$

Here χ_s represents a p_z orbital on atom s (Warshel & Parson, 1987). In this representation, the off-diagonal matrix elements

for resonance interactions in P^+ take the form

$$U_{P_L^+P_M^+} \equiv \langle P_L^+|\mathcal{H}|P_M^+\rangle \approx -\sum_s\sum_t \nu_s^{P_L}\nu_t^{P_M}\beta_{s,t} \quad (3)$$

where $\beta_{s,t}$ is the atomic resonance integral between atom s of P_L and atom t of P_M, $\nu_s^{P_L}$ are the expansion coefficients (eq 2) for the HOMO of P_L, and $\nu_t^{P_M}$ are the corresponding coefficients for P_M. The resonance integrals $\beta_{s,t}$ can be expressed as semiempirical functions of the interatomic distances and the orientations of the two molecules (Warshel & Parson, 1987; Parson & Warshel, 1987). For the *Rp. viridis* crystal structure, $U_{P_L^+P_M^+}$ is calculated to be about −910 cm^{-1} (Parson et al., 1990). Similar calculations using the *Rb. sphaeroides* crystal structure give $U_{P_L^+P_M^+} \approx -495$ cm^{-1}. Although the center-to-center distance between P_L and P_M is almost the same in the crystal structures for the two species, $|U_{P_L^+P_M^+}|$ is larger in *Rp. viridis* because the two BChls are closer together where they overlap in ring I.

Diagonalizing the 2 × 2 U matrix gives two eigenstates, Ψ_a and Ψ_b:

$$\Psi_a = \left(\frac{1+c}{2}\right)^{1/2}P_L^+ + \left(\frac{1-c}{2}\right)^{1/2}P_M^+$$

and

$$\Psi_b = \left(\frac{1-c}{2}\right)^{1/2}P_L^+ - \left(\frac{1+c}{2}\right)^{1/2}P_M^+ \quad (4)$$

with

$$c = \frac{\delta}{[\delta^2 + 4(U_{P_L^+P_M^+})^2]^{1/2}} \quad (5)$$

where δ is the gap between the energies of the two basis states. The eigenstates are separated in energy by

$$\Delta E = [\delta^2 + 4(U_{P_L^+P_M^+})^2]^{1/2} \quad (6)$$

[See, for example, Förster (1965) and Shipman et al. (1976) for other formulations of essentially the same expressions.] The negative values of $U_{P_L^+P_M^+}$ calculated for the RC put Ψ_a below Ψ_b in energy. In a "supermolecule"[2] picture of the BChl dimer, Ψ_a corresponds to populating a bonding molecular orbital of the dimer, and Ψ_b an antibonding orbital. We shall show that the properties of the 2600-cm^{-1} band are consistent with an excitation of P^+ from Ψ_a to Ψ_b.

The transition dipole for an excitation from Ψ_a to Ψ_b is

$$\begin{aligned}\vec{\mu}_{a\,b} &\equiv \langle\Psi_b|\tilde{\vec{\mu}}|\Psi_a\rangle \\ &\approx \frac{[(1+c)(1-c)]^{1/2}}{2}(\langle P_L^+|\tilde{\vec{\mu}}|P_L^+\rangle - \langle P_M^+|\tilde{\vec{\mu}}|P_M^+\rangle) \\ &\approx \frac{[(1+c)(1-c)]^{1/2}}{2}e(\vec{R}_{P_M} - \vec{R}_{P_L}) \end{aligned} \quad (7)$$

where $\tilde{\vec{\mu}}$ is the dipole-moment operator, e is the charge of an electron, and $\vec{R}_{P_M}$ and $\vec{R}_{P_L}$ are the centers of the HOMOs of P_M and P_L. Cross terms of the type $\langle P_L^+|\tilde{\vec{\mu}}|P_M^+\rangle$ do not contribute significantly to $\vec{\mu}_{a\,b}$ because P_L and P_M have no atoms in common.

[2] In a supermolecule picture, the bonding orbital would be located largely between the two BChls; the antibonding orbital, more peripherally. These different spatial distributions could result in different interactions of the dimer with its surroundings, and a supermolecule treatment might include an additional contribution to ΔE reflecting this effect. In a dimer with rotational symmetry the effect probably is relatively small, because the redistribution of electron density causes little or no change in dipole moment.

If the energies of P_L^+ and P_M^+ are similar [$\delta^2 \ll 4(U_{P_L^+P_M^+})^2$], c will be close to zero. The eigenstates then will be simply symmetric and antisymmetric combinations of the basis states:

$$\Psi_a = 2^{-1/2}P_L^+ + 2^{-1/2}P_M^+$$

$$\Psi_b = 2^{-1/2}P_L^+ - 2^{-1/2}P_M^+ \quad (8)$$

The energy difference between the eigenstates is $2|U_{P_L^+P_M^+}|$, and the transition dipole becomes

$$\vec{\mu}_{a\,b} \approx \frac{1}{2}e(\vec{R}_{P_M} - \vec{R}_{P_L}) = \frac{4.803\ D}{2}(\vec{R}_{P_M} - \vec{R}_{P_L})/Å \quad (9)$$

The magnitude of the transition dipole for a dimer with 2-fold symmetry thus is expected to be approximately half the dipole moment created by moving an electron from one BChl to the other. For either *Rp. viridis* or *Rb. sphaeroides*, this would give a dipole strength ($|\vec{\mu}_{a\,b}|^2$) of about 300 D^2. The absorption transition would be polarized along the vector connecting the centers of P_L and P_M, which is perpendicular to the pseudosymmetry axis of the RC. But note that the excitation from Ψ_a to Ψ_b is not fundamentally a charge-transfer transition. Its dipole strength arises entirely from terms in which the positively charged hole is on the same molecule in Ψ_a and Ψ_b (eq 7). If the energies of P_L^+ and P_M^+ differ substantially so that the hole tends to localize on one molecule in Ψ_a and on the other molecule in Ψ_b ($\delta^2 \gg 4(U_{P_L^+P_M^+})^2$), c approaches 1.0 and the dipole strength goes to zero.

The magnitude of δ cannot yet be calculated reliably for the RC because it is sensitive to long-range electrostatic interactions of the BChls with the protein and to molecular structural distortions that probably are beyond the resolution of the crystal structures (Parson et al., 1990). Although the structural distortions that are seen in the X-ray structures appear to favor P_L^+ relative to P_M^+ (Barkigia et al., 1988; Lendzian et al., 1988; Plato et al., 1988a,b), electrostatics calculations based on the *Rp. viridis* crystal structure suggest that, in this species, P_M^+ lies below P_L^+ by 3.0–5.3 kcal/mol (1100–1900 cm^{-1}) (Parson et al., 1990). However, these calculations were based on the crystal structure of unoxidized RCs. Reorganization of the protein in the more stable eigenstate of P^+ would increase the absolute magnitude of δ.

Equations 5–7 can be solved for both $|U_{P_L^+P_M^+}|$ and $|\delta|$ by using the crystallographic value of ($\vec{R}_{P_L} - \vec{R}_{P_M}$) and the measured ΔE and $|\vec{\mu}_{a\,b}|^2$. Figure 5 shows $|U_{P_L^+P_M^+}|$ and $|\delta|$ as functions of $|\vec{\mu}_{a\,b}|^2$ for several values of ΔE. The experimental results for *Rb. sphaeroides* ($\Delta E = 2600 \pm 100$ cm^{-1} and $|\vec{\mu}_{a\,b}|^2 = 25 \pm 8$ D^2) yield $|U_{P_L^+P_M^+}| = 380 \pm 70$ cm^{-1} and $|\delta| = 2490 \pm 150$ cm^{-1}. (For simplicity, we have taken ΔE to be the wavenumber at the absorption maximum, rather than attempting to estimate the 0–0 transition energy. Decreasing ΔE by 500 cm^{-1} would lower $|U_{P_L^+P_M^+}|$ by 70 and $|\delta|$ by 480 cm^{-1}.) The measurements on *Rp. viridis* ($\Delta E = 2750 \pm 100$ cm^{-1} and $|\vec{\mu}_{a\,b}|^2 = 85 \pm 28$ D^2) give $|U_{P_L^+P_M^+}| = 730 \pm 130$ and $|\delta| = 2330 \pm 150$ cm^{-1}. Considering the simplicity of the theoretical model, the value of $|U_{P_L^+P_M^+}|$ for each species appears to agree acceptably with the value calculated on the basis of the crystal structure using eq 3 (495 cm^{-1} in *Rb. sphaeroides*, 910 cm^{-1} in *Rp. viridis*). The values of $|\delta|$ also seem not unreasonable, in the light of the electrostatics calculations on *Rp. viridis*.

Both the energy and dipole strength of the new transition thus appear to be consistent with an excitation of P^+ from Ψ_a to Ψ_b. This assignment is strengthened by the observation

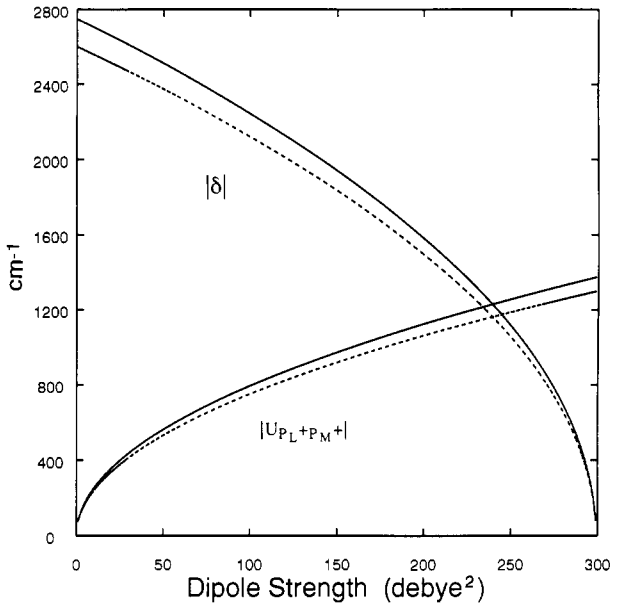

FIGURE 5: Calculated magnitudes of the interaction matrix element ($|U_{P_L^+P_M^+}|$) and energy difference ($|\delta|$) between the P_L^+ and P_M^+ basis states, as functions of the dipole strength ($|\vec{\mu}_{a\,b}|^2$) and transition energy (ΔE) of the mid-IR absorption band of P^+. The curves were calculated by rearranging eqs 5–7 to cast the experimentally measurable quantities $|\vec{\mu}_{a\,b}|^2$ and ΔE as the independent variables: solid curves, ΔE = 2750 cm^{-1}; dotted curves, ΔE = 2600 cm^{-1}.

that the transition dipole is oriented at an angle of at least 60° with respect to the pseudosymmetry axis of the RC. (The predicted angle is 90°.) The large width of the absorption band also is qualitatively consistent with this interpretation, because of the expected dependence of δ on electrostatic interactions with the protein and the sensitivity of both $U_{P_L^+P_M^+}$ and $(\vec{R}_{P_L} - \vec{R}_{P_M})$ to small changes in the positions of P_L and P_M. These dependencies should couple the transition strongly to vibrational motions of the protein and the pigments. In addition, variations in structural parameters should result in inhomogeneous broadening of the band. Finally, the loss or strong attenuation of the absorption band in the heterodimer mutants is predicted by eqs 5 and 7, which show that a highly asymmetrical dimer with a large value of $|\delta|$ will have a very small dipole strength.

The general agreement between the calculated and observed spectroscopic properties suggests that eq 3 provides a good framework for evaluating the magnitudes of resonance interactions between P_L and P_M. The underlying parametrization of the atomic resonance integrals appears to work well for both *Rb. sphaeroides* and *Rp. viridis* RCs, in spite of the differences between the crystal structures for the two species. However, the simplifications inherent in the theory described above limit the accuracy of the values of $|\delta|$ and $U_{P_L^+P_M^+}$ that we have extracted from Figure 5. For example, the dipole operator that is used in eq 7 often leads to overestimates of calculated dipole strengths for planar conjugated molecules. The transition gradient operator frequently gives more accurate results.

Because the theory that we have used here considers only the HOMOs of P_L and P_M, it applies only to the lowest-energy electronic absorption band of P^+. The theory thus is silent with regard to the band in the 1300-nm region, and it neglects configuration interactions with this and other transitions. As will be discussed elsewhere (Parson et al., 1992), the 1300-nm band probably reflects excitation to a state in which the hole resides predominantly in ϕ_1 of the four-orbital model. Again, there are two basis states of this nature, which are mixed by resonance interactions between the BChls. Configuration interactions with transitions to these states and with the Q_y, Q_x, and Soret transitions of the BChls tend to decrease the predicted dipole strength of the 2600-cm^{-1} band. In a more complete theory that includes configuration interactions and also considers possible changes in the molecular orbitals caused by hydrogen bonding of the BChl acetyl groups, the energy and dipole strength of the mid-IR band for *Rp. viridis* RCs are fit well by taking $|\delta|$ to be 1900 ± 150 cm^{-1}, which is about 400 cm^{-1} below the value suggested above. This estimate of $|\delta|$ would be reduced by approximately an additional 500 cm^{-1} if we put ΔE at the energy of the shoulder on the low-energy side of the band instead of at the peak.

The conclusion that there is a difference of 1800–2000 cm^{-1} between the energies of the basis states P_L^+ and P_M^+ is consistent with the large Stark effect seen in the long-wavelength absorption band of P (Lockhart & Boxer, 1987, 1988; Lösche et al., 1987). The Stark effect indicates that excitation to P* involves a substantial change in dipole moment, most likely because the excited state includes contributions from a charge-transfer state in which an electron moves from P_L to P_M ($P_L^+P_M^-$) or vice versa ($P_M^+P_L^-$). It is unclear which of the two charge-transfer states is the more important in this regard. However, these states evidently differ significantly in energy, because if they were isoenergetic their opposite contributions to the change in dipole moment would cancel (Parson & Warshel, 1987).

The ENDOR and EPR spectra of P^+ also appear to be consistent with an asymmetric distribution of the charge between P_L and P_M in the case of *Rp. viridis*, but suggest that in *Rb. sphaeroides* the distribution is more nearly equal (Katz et al., 1979; Davis et al., 1979; Lendzian et al., 1988, 1990; Norris et al., 1989; Plato et al., 1988a,b; Lous et al., 1990). Our results and the Stark measurements suggest that the distribution is asymmetrical in both species. The reason for the apparent discrepancy with the magnetic resonance spectra in the case of *Rb. sphaeroides* is unclear. However, an asymmetry in the charge distribution in this species seems consistent with the crystallographic result that the interactions of P_L and P_M with the surrounding amino acid residues are, if anything, more asymmetrical in *Rb. sphaeroides* than in *Rp. viridis* (Deisenhofer & Michel, 1989a; Allen et al., 1987; Yeates et al., 1988; Chang et al., 1991; El-Kabbani et al., 1991).

Another observation that seems difficult to reconcile with a highly asymmetric charge distribution in P^+ is that the midpoint redox potential (E_m) of P differs by only about 0.03 V between the two *Rb. sphaeroides* heterodimer mutants, in which either P_L or P_M is replaced by BPh [Davis et al. (1992); C. Schenck, personal communication]. We might have expected the E_m to be particularly sensitive to modifications of the pigment that holds the larger positive charge in P^+. Further structural and computational studies of such mutant RCs should be informative.

Duchowski and Bocian (1990a–c) and Perng et al. (1990, 1991) have described strong near-IR absorption bands of cationic sandwich compounds in which two porphyrins share a single lanthanide ion. They attributed these bands to an excitation of the dimer supermolecule from a bonding to an antibonding orbital. In the lanthanide complexes, the bands occur between 8000 and 9000 cm^{-1}. Resonance interactions probably are considerably stronger in these complexes than in P^+ because the macrocyclic rings have more extensive overlap. Similar near-IR bands are seen in the excited triplet

states of Hf^{IV}- and Zr^{IV}-porphyrin sandwich complexes (Bilsel et al., 1991).

A striking feature of the spectra of the lanthanide sandwich complexes is a strong coupling to a vibrational mode of about 300 cm^{-1} (Duchowski & Bocian, 1990a–c; Perng et al., 1990, 1991). The long-wavelength absorption band of P is coupled to a characteristic "marker mode" that probably reflects an intermolecular vibrational mode of P; this vibration has an energy of about 135 cm^{-1} in *Rp. viridis* and about 115 cm^{-1} in *Rb. sphaeroides* (Klevanik et al., 1988; Shuvalov et al., 1988; Johnson et al., 1989, 1990; Middendorf et al., 1991). Although the 2600-cm^{-1} absorption band of P^+ does not have a well-resolved vibronic structure, it does appear to have a shoulder located about 500 cm^{-1} below the absorption maximum. Equation 7 suggests that the absorption would be strongly coupled to intermolecular vibrations that modulate the distance between P_L and P_M. Oxidation of P would be expected to decrease the repulsion between the two BChls (Warshel, 1980) and might shift intermolecular vibrational modes to higher energies.

Considering the likely dependence of the 2600-cm^{-1} band on the interactions between P_L and P_M, the observation that the position and relative intensity of the band are not very sensitive to temperature indicates that the intermolecular distance in P^+ probably does not change significantly when RCs are cooled. A change in the distance between the BChls has been suggested as a possible explanation for the temperature dependence of the long-wavelength absorption band of P (Scherer et al., 1985; Parson & Warshel, 1987; Kirmaier & Holten, 1988; Lous & Hoff, 1989; Won & Friesner, 1988b).

ACKNOWLEDGMENT

We thank Drs. M. Schiffer for providing the crystallographic coordinates for the *Rb. sphaeroides* RC, J. Deisenhofer for those of *Rp. viridis*, D. Thibodeau for measuring the linear dichroism spectra, S. Robles and D. Youvan for providing *Rb. capsulatus* cells, and C. Schenck, L. Shipman, W. Mäntele, V. Nagarajan, and A. Warshel for helpful discussions.

REFERENCES

Allen, J. P., Feher, G., Yeates, T. O., Komiya, H., & Rees, D. C. (1987) *Proc. Natl. Acad. Sci. U.S.A. 84*, 6162–6166.

Barkigia, K. M., Chantranupong, L., Smith, K. M., & Fajer, J. (1988) *J. Am. Chem. Soc. 110*, 7566–7567.

Bilsel, O., Buchler, J. W., Hammerschmitt, P., Rodriguez, J., & Holten, D. (1991) *Chem. Phys. Lett. 182*, 415–421.

Breton, J. (1985) *Biochim. Biophys. Acta 810*, 235–245.

Breton, J., & Verméglio, A., Eds. (1988) *The Photosynthetic Bacterial Reaction Center*, Plenum, New York.

Breton, J., Martin, J.-L., Petrich, J., Migus, A., & Antonetti, A. (1986) *FEBS Lett. 209*, 37–43.

Breton, J., Thibodeau, D. L., Berthomieu, C., Mäntele, W., Verméglio, A., & Nabedryk, E. (1991a) *FEBS Lett. 278*, 257–260.

Breton, J., Berthomieu, C., Thibodeau, D. L., & Nabedryk, E. (1991b) *FEBS Lett. 288*, 109–113.

Breton, J., Bylina, E. J., Robles, S. J., Youvan, D. C., & Nabedryk, E. (1991c) *Biophys. J. 59*, 31A.

Breton, J., Nabedryk, E., & Parson, W. W. (1992) *Biophys. J. 61*, A101.

Buchanan, S., Michel, H., & Gewert, K. (1990) in *Reaction Centers of Photosynthetic Bacteria* (Michel-Beyerle, M. E., Ed.) pp 75–85, Springer, Berlin.

Chang, C.-H., El-Kabbani, O., Tiede, D., Norris, J., & Schiffer, M. (1991) *Biochemistry 30*, 5352–5360.

Clayton, R. K., & Clayton, B. J. (1978) *Biochim. Biophys. Acta 501*, 478–487.

Coleman, W. J., & Youvan, D. C. (1990) *Annu. Rev. Biophys. Biophys. Chem. 19*, 333–367.

Davis, D., Dong, A., Caughey, W. S., & Schenck, C. C. (1992) *Biophys. J. 61*, A153.

Davis, M. S., Forman, A., Hanson, L. K., Thornber, J. P., & Fajer, J. (1979) *J. Phys. Chem. 83*, 3325–3332.

Deisenhofer, J., & Michel, H. (1989a) *Science 245*, 1463–1473.

Deisenhofer, J., & Michel, H. (1989b) *EMBO J. 8*, 2149–2169.

Deisenhofer, J., Epp, O., Miki, K., Huber, R., & Michel, H. (1985) *Nature 318*, 618–624.

Duchowski, J. K., & Bocian, D. F. (1990a) *J. Am. Chem. Soc. 112*, 3312–3316.

Duchowski, J. K., & Bocian, D. F. (1990b) *Inorg. Chem. 29*, 4158–4160.

Duchowski, J. K., & Bocian, D. F. (1990c) *J. Am. Chem. Soc. 112*, 8807–8811.

Dutton, P. L., Kaufmann, K. J., Chance, B., & Rentzepis, P. M. (1975) *FEBS Lett. 60*, 275–280.

Eccles, J., & Honig, B. (1983) *Proc. Natl. Acad. Sci. U.S.A. 80*, 4959–4962.

Eccles, J., Honig, B., & Schulten, K. (1988) *Biophys. J. 53*, 137–144.

El-Kabbani, O., Chang, C.-H., Tiede, D., Norris, J., & Schiffer, M. (1991) *Biochemistry 30*, 5361–5369.

Fajer, J., Brune, D. C., Davis, M. S., Forman, A., & Spaulding, L. D. (1975) *Proc. Natl. Acad. Sci. U.S.A. 72*, 4956–4960.

Feher, G., & Okamura, M. Y. (1978) in *The Photosynthetic Bacteria* (Clayton, R. K., & Sistrom, W. R., Eds.) pp 349–386, Plenum Press, New York.

Feher, G., Allen, J. P., Okamura, M. Y., & Rees, D. C. (1989) *Nature 339*, 111–116.

Förster, T. (1965) in *Modern Quantum Chemistry* (Sinanoglu, O., Ed.) Vol. III, pp 93–137, Academic Press, New York.

Friesner, R. A., & Won, Y. (1989) *Biochim. Biophys. Acta 977*, 99–122.

Gouterman, M. P. (1959) *J. Chem. Phys. 30*, 1139–1161.

Hanson, L. K. (1988) *Photochem. Photobiol. 47*, 903–921.

Holzapfel, W., Finkele, U., Kaiser, W., Oesterhelt, D., Scheer, H., Stiltz, U., & Zinth, W. (1990) *Proc. Natl. Acad. Sci. U.S.A. 87*, 5168–5172.

Johnson, S. G., Tang, G., Jankowiak, R., Hayes, J. M., Small, G. J., & Tiede, D. M. (1989) *J. Phys. Chem. 93*, 5953–5957.

Johnson, S. G., Tang, G., Jankowiak, R., Hayes, J. M., Small, G. J., & Tiede, D. M. (1990) *J. Phys. Chem. 94*, 5850–5855.

Källebring, B., & Larsson, S. (1987) *Chem. Phys. Lett. 138*, 76–82.

Katz, J. J., Shipman, L. L., & Norris, J. R. (1979) *Ciba Found. Symp. 61*, 1–34.

Kirmaier, C., & Holten, D. (1987) *Photosynth. Res. 13*, 225–260.

Kirmaier, C., & Holten, D. (1988) in *The Photosynthetic Bacterial Reaction Center* (Breton, J., & Verméglio, A., Eds.) pp 219–228, Plenum Press, New York.

Klevanik, A. V., Ganago, A. O., Shkuropatov, A. Ya., & Shuvalov, V. A. (1988) *FEBS Lett. 237*, 61–64.

Kuhn, H. (1986) *Phys. Rev. A 34*, 3409–3425.

Lendzian, F., Lubitz, W., Scheer, H., Hoff, A. J., Plato, M., Tränkle, E., & Möbius, K. (1988) *Chem. Phys. Lett. 148*, 377–385.

Lendzian, F., Endeward, B., Plato, M., Bumann, S., Lubitz, W., & Möbius, K. (1990) in *Reaction Centers of Photosynthetic Bacteria* (Michel-Beyerle, M. E., Ed.) pp 57–68, Springer, Berlin.

Lockhart, D. J., & Boxer, S. G. (1987) *Biochemistry 26*, 664–668.

Lockhart, D. J., & Boxer, S. G. (1988) *Chem. Phys. Lett. 144*, 243–250.

Lösche, M., Feher, G., & Okamura, M. Y. (1987) *Proc. Natl. Acad. Sci. U.S.A. 84*, 7537–7541.

Lous, E. J., & Hoff, A. J. (1989) *Biochim. Biophys. Acta 974*, 88–103.

Lous, E. J., Huber, M., Isaacson, R. A., & Feher, G. (1990) in *Reaction Centers of Photosynthetic Bacteria* (Michel-Beyerle, M. E., Ed.) pp 45–55, Springer, Berlin.
Mäntele, W., Nabedryk, E., Tavitian, B. A., Kreutz, W., & Breton, J. (1985) *FEBS Lett. 187*, 227–232.
Mäntele, W., Wollenweber, A., Nabedryk, E., & Breton, J. (1988) *Proc. Natl. Acad. Sci. U.S.A. 85*, 8468–8472.
Martin, J.-L., Breton, J., Hoff, A. J., Migus, A., & Antonetti, A. (1986) *Proc. Natl. Acad. Sci. U.S.A. 83*, 5121–5125.
Michel-Beyerle, M.-E., Ed. (1990) *Reaction Centers of Photosynthetic Bacteria*, Springer, Berlin.
Middendorf, T. R., Mazzola, L. T., Gaul, D. F., Schenck, C. C., & Boxer, S. G. (1991) *J. Phys. Chem. 95*, 10142–10151.
Nabedryk, E., Mäntele, W., Tavitian, B. A., & Breton, J. (1986) *Photochem. Photobiol. 43*, 461–465.
Nabedryk, E., Andrianambinintsoa, S., Mäntele, W., & Breton, J. (1988) in *The Photosynthetic Bacterial Reaction Center* (Breton, J., & Verméglio, A., Eds.) pp 237–250, Plenum, New York.
Nabedryk, E., Bagley, K. A., Thibodeau, D. L., Bauscher, M., Mäntele, W., & Breton, J. (1990) *FEBS Lett. 266*, 59–62.
Nabedryk, E., Berthomieu, C., Verméglio, A., & Breton, J. (1991) *FEBS Lett. 293*, 53–58.
Nabedryk, E., Robles, S. J., Goldman, E., Youvan, D. C., & Breton, J. (1992) *Biophys. J. 61*, A101.
Norris, J. R., Budil, D. E., Gast, P., Chang, C.-H., El-Kabbani, O., & Schiffer, M. (1989) *Proc. Natl. Acad. Sci. U.S.A. 86*, 4335–4339.
Parson, W. W., & Cogdell, R. J. (1975) *Biochim. Biophys. Acta 416*, 105–106.
Parson, W. W., & Warshel, A. (1987) *J. Am. Chem. Soc. 109*, 6152–6163.
Parson, W. W., Creighton, S., & Warshel, A. (1987) in *Primary Reactions of Photobiology* (Kobayashi, T., Ed.) pp 43–51, Springer-Verlag, Berlin.
Parson, W. W., Chu, Z.-T., & Warshel, A. (1990) *Biochim. Biophys. Acta 1017*, 251–272.
Parson, W. W., Nabedryk, E., & Breton, J. (1992) in *The Photosynthetic Reaction Centre: Structure, Spectroscopy and Dynamics* (Breton, J., & Verméglio, A., Eds.) Plenum, New York (in press).
Perng, J.-H., Duchowski, J. K., & Bocian, D. F. (1990) *J. Phys. Chem. 94*, 6684–6691.
Perng, J.-H., Duchowski, J. K., & Bocian, D. F. (1991) *J. Phys. Chem. 95*, 1319–1323.
Philipson, K. D., & Sauer, K. (1973) *Biochemistry 12*, 535–539.
Plato, M., & Winscom, C. J. (1988) in *The Photosynthetic Bacterial Reaction Center* (Breton, J., & Verméglio, A., Eds.) pp 421–424, Plenum Press: New York.
Plato, M., Lubitz, W., Lendzian, F., Tränkle, E., & Möbius, K. (1988a) *Isr. J. Chem. 28*, 109–119.
Plato, M., Möbius, K., Michel-Beyerle, M. E., Bixon, M., & Jortner, J. (1988b) *J. Am. Chem. Soc. 110*, 7279–7285.
Scherer, P. O. J., & Fischer, S. F. (1989a) *Chem. Phys. 131*, 115–127.
Scherer, P. O. J., & Fischer, S. F. (1989b) *J. Phys. Chem. 93*, 1633–1637.
Scherer, P. O. J., & Fischer, S. F. (1991) in *Chlorophylls* (Scheer, H., Ed.) pp 1079–1093, CRC Press, Boca Raton, FL.
Scherer, P. O. J., Fischer, S. F., Hörber, J. K. H., Michel-Beyerle, M. E., & Michel, H. (1985) in *Antennas and Reaction Centers of Photosynthetic Bacteria* (Michel-Beyerle, M. E., Ed.) pp 131–137, Springer-Verlag, Berlin.
Scherz, A., & Parson, W. W. (1985) *Biochim. Biophys. Acta 766*, 666–678.
Shipman, L. L., Norris, J. R., & Katz, J. (1976) *J. Phys. Chem. 80*, 877–882.
Shuvalov, V. A., Klevanik, A. V., Ganago, A. O., Shkuropatov, A. Ya., & Gubanov, V. S. (1988) *FEBS Lett. 237*, 57–60.
Straley, S. C., Parson, W. W., Mauzerall, D. C., & Clayton, R. K. (1973) *Biochim. Biophys. Acta 305*, 597–609.
Thibodeau, D. L., Breton, J., Berthomieu, C., Bagley, K. A., & Mäntele, W., & Nabedryk, E. (1990) in *Reaction Centers of Photosynthetic Bacteria* (Michel-Beyerle, M. E., Ed.) pp 87–98, Springer, Berlin.
Thibodeau, D. L., Nabedryk, E., & Breton, J. (1991) in *Spectroscopy of Biological Molecules* (Hester, R. E., & Girling, R. B., Eds.) pp 69–70, Royal Society of Chemistry, Cambridge, England.
Thompson, M. A., & Zerner, M. C. (1990) *J. Am. Chem. Soc. 112*, 7828–7830.
Tiede, D. M., Budil, D. E., Tang, J., El-Kabbani, O., & Norris, J. R. (1988) in *The Photosynthetic Bacterial Reaction Center* (Breton, J., & Verméglio, A., Eds.) pp 13–20, Plenum, New York.
Warshel, A. (1980) *Proc. Natl. Acad. Sci. U.S.A. 77*, 3105–3109.
Warshel, A., & Parson, W. W. (1987) *J. Am. Chem. Soc. 109*, 6143–6152.
Warshel, A., Creighton, S., & Parson, W. W. (1988) *J. Phys. Chem. 92*, 2696–2701.
Won, Y., & Friesner, R. A. (1988a) *J. Phys. Chem. 92*, 2208–2214.
Won, Y., & Friesner, R. A. (1988b) *Isr. J. Chem. 28*, 67–72.
Woodbury, N. W., Becker, M., Middendorf, D., & Parson, W. W. (1985) *Biochemistry 24*, 7516–7521.
Yeates, T. O., Komiya, H., Chirino, A., Rees, D. C., Allen, J. P., & Feher, G. (1988) *Proc. Natl. Acad. Sci. U.S.A. 85*, 7993–7997.
Zundel, G. (1988) *J. Mol. Struct. 177*, 43–68.